EVALUATION OF FLEXURAL MODULUS OF ULTRA-THIN CHOPPED CARBON FIBER TAPE REINFORCED THERMOPLASTICS

Y. Nakashima[1], H. Suganuma[1], S. Yamashita[1] and J. Takahashi[1]

[1]Department of Systems Innovation, School of Engineering, The University of Tokyo,
7-3-1 Hongo, Bunkyo-ku, Tokyo 113-8656, JAPAN
Email: nakashima-yuto@cfrtp.t.u-tokyo.ac.jp

Keywords: Automobile, UT-CTT, Randomly oriented strands, Flexural modulus, Variance

Abstract
Although ultra-thin chopped carbon fiber tape reinforced thermoplastics (UT-CTT), which are a kind of randomly oriented strands (ROS) made by water dispersed thin tape, were successfully developed recently because of their high mechanical properties, test results by small specimens tend to be somewhat scattered. Therefore to evaluate their properties accurately, an analytical model for the mean value and the variance of the tensile modulus of ROS with chopped tapes has been proposed in a previous study. A model for the flexural modulus of ROS with chopped tapes has also been proposed but has not shown good agreement on account of out-of-plane shear deflection. Thus, in this study, a modified model was proposed and verified by comparison with experimental results. In order to obtain the experimental flexural modulus, both 3-point bending test and 4-point bending test were carried out. And each of the support span or the thickness of specimens was varied in these tests. After the comparison, it was found that the prediction results by the model showed good agreement with experimental results. This study enabled to evaluate the scatter and the effect of out-of-plane shear deflection without experiments.

1. Introduction

Since randomly oriented strands (ROS) are the promising materials for primary structures of mass-produced automobiles thanks to their high mechanical properties and suitability for complex shape, a number of studies, such as on failure modes [1] and molding [2,3], have been conducted [4-6]. However, since these materials contain several centimeters of chopped carbon fiber tapes, test results by small specimens tend to be highly scattered [1,7]. This characteristic has made evaluating such materials difficult and prevented an extension of their application range. Therefore, ROS with smaller scattered properties had been desired and ultra-thin carbon fiber tape reinforced thermoplastics (UT-CTT), which are ROS manufactured by water dispersion of chopped ultra-thin prepreg, have been successfully developed in Japanese national project. The properties of these materials, however, follow statistical distributions caused by the manufacturing process, so they are more or less scattered even in UT-CTT. Hence in order to evaluate their properties accurately, to secure reliability and to design structures efficiently, a prediction model is sure to be necessary. Feraboli et al. [8] divided a specimen into regions and regarded a region as laminates with continuous plies. Selezneva et al. [9] modeled a 2D-FE specimen in which randomly placed and oriented strands are generated. In these studies though each discretized element could be calculated in a short time, stress-strain response was focused on and a property of a whole specimen was simulated by finite element method (FEM). Sato et al. [7] and Zhang [10] proposed a model by which an entire tensile modulus can be calculated in Monte Carlo simulation rather than FEM to quantify its scatter through the repeat of the calculation many times, while have not proposed a model for flexural modulus yet. The goal of this study is to propose a flexural model that captures the scatter of flexural modulus of ROS.

Excerpt from ISBN 978-3-00-053387-7

2. Analytical model

2.1. Modeling process in previous study [10]

In this part, the summary of a previous study by Zhang [10] will be shown. ROS with chopped tapes are composed of several centimeters of randomly dispersed tapes. Therefore, it is assumed that both the location and the orientation of each tape are given completely randomly. This characteristic causes that these tapes make small gaps by overlapping each other as shown in Fig. 1 (a). These gaps can be resin-rich areas or defects and are difficult to be reproduced in simulation. However, when it is to reveal the statistical characteristic of macro-scale property such as flexural modulus that the main purpose is, an efficient analytical model which ignores these resin-rich areas and defects is more useful than a specific model which can acquire all overlap of tapes. Hence, in the analytical model, each tape is transformed to a square ply having the information of size and orientation of the tape and this square ply is laid in an imaginary specimen without overlapping. Exactly speaking, edge length of equivalent square ply is $\sqrt{lw}$ where l is the length and w is the width of tape (Fig. 1 (b)). In that case, it is important that the number of tapes in a specimen is maintained because the area of an equivalent square ply is same to a tape. Moreover, the orientation angle of a tape to the global longitudinal axis, θ, is inherited to the fiber orientation in an equivalent square ply, while the square itself remains orthogonal to global coordinate system as shown in Fig. 1 (b).

The global coordinate system is defined that x is the longitudinal axis, y is the transverse axis and z is the out-of-plane axis. The flexural modulus along x-axis of an equivalent square ply is calculated as follows:

$$E_k = \left(\frac{\cos^4\theta}{E_1} + \frac{\sin^4\theta}{E_2} + \frac{\sin^2\theta\cos^2\theta}{G_{12}} - 2\nu_{12}\frac{\sin^2\theta\cos^2\theta}{E_1} \right)^{-1} \tag{1}$$

where E_1 and E_2 are the Young's moduli of $0°$ direction and $90°$ direction, ν_{12} is the Poisson's ratio and G_{12} is the in-plane shear modulus of a unidirectional (UD) tape. Furthermore, the relation between stress and strain can be expressed using a stiffness matrix $\overline{\mathbf{C}} = \left[\overline{C}_{ij}\right]$ as below:

$$\begin{bmatrix} \sigma_x \\ \sigma_y \\ \tau_{xy} \end{bmatrix} = \begin{bmatrix} \overline{C}_{11} & \overline{C}_{12} & \overline{C}_{16} \\ \overline{C}_{12} & \overline{C}_{22} & \overline{C}_{26} \\ \overline{C}_{16} & \overline{C}_{26} & \overline{C}_{66} \end{bmatrix} \begin{bmatrix} \varepsilon_x \\ \varepsilon_y \\ \gamma_{xy} \end{bmatrix} \tag{2}$$

The equivalent square plies are compounded to make an imaginary specimen. The compounding process is conducted along z-axis, y-axis and x-axis, and finally the flexural modulus along x-axis is obtained.

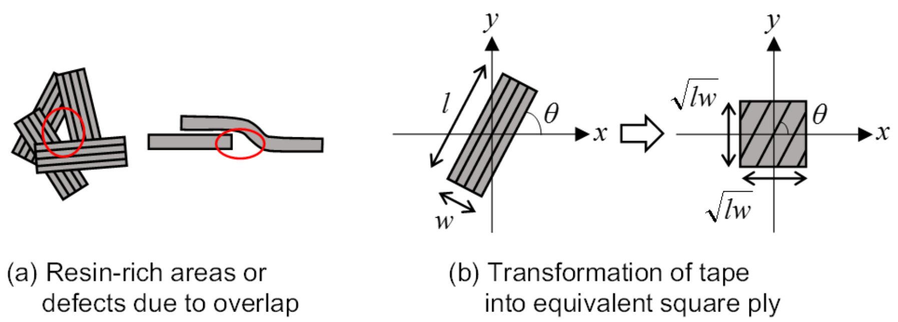

Fig. 1 Assumption in modeling [10].

Excerpt from ISBN 978-3-00-053387-7

2.2. Modified model for flexural modulus

2.2.1. Modified 3-point bending model

The model for 3-point bending proposed by Zhang didn't show good agreement with experimental results [10]. Generally speaking, out-of-plane shear deflection appears in 3-point bending and it is added to bending deflection. Thus, the conventional model for flexural modulus is modified to quantify the effect of shear deflection.

The mid-span deflection in 3-point bending δ is described as follows:

$$\delta = \delta_1 + \delta_{13} = \frac{PL^3}{48E_1 I} + \frac{3PL}{8G_{13}A} = \delta_1\left[1 + \frac{3}{2}\left(\frac{T}{L}\right)^2 \frac{E_1}{G_{13}}\right] \tag{3}$$

where P is the applied force, E_1 is the pure flexural modulus, I is the moment of inertia of area, A is the sectional area and G_{13} is the out-of-plane shear modulus. The first term expresses bending deflection δ_1 and the second term expresses out-of-plane shear deflection δ_{13}. Since elastic modulus is proportional to the reciprocal of deflection, the flexural modulus for 3-point bending E_b is given by

$$\frac{1}{E_b} = \frac{\delta}{\delta_1}\cdot\frac{1}{E_1} = \frac{1}{E_1} + \frac{3}{2}\left(\frac{T}{L}\right)^2 \frac{1}{G_{13}} \tag{4}$$

The conventional model outputs the pure flexural modulus because it assumes the pure bending condition without shear deflection. Hence, in the modified model, E_b is calculated by the equation (4) after the calculation of E_1. Even though G_{13} is somewhat scattered, it is inferred that the scatter is much smaller than that of E_1 so G_{13} can be considered the constant.

2.2.2. 4-point bending model

Two types of bending test, that is, 3-point and 4-point bending test, are widely used to estimate some mechanical properties. As mentioned above, the out-of-plane shear deflection causes an underestimation of flexural modulus and this effects is larger in 3-point bending than in 4-point bending. Therefore, a new model for 4-point bending will be proposed. The load span is determined as $L/2$.

The calculation process is almost same to 3-point bending. The process of compounding equivalent square plies is conducted along *z*-axis, *y*-axis and *x*-axis. The second step makes a part aligned in a row and the third step will be explained as follows. In 4-point bending, the beam can be divided into two parts which can be regarded as cantilevers of which force $P/2$ is applied at the end and center, as shown in Fig. 2. There are two loads and it results that the elastic curve equation isn't determined uniquely because the bending moment is proportional to *x* in $0 \le x \le L/4$ while it is constant in $L/4 \le x \le L/2$. A solution to this problem is to divide a cantilever into two parts again. Two types of elastic curve equation are solved in each condition and these solutions are combined by the boundary condition at $x = L/4$. Two equations are described as follows:

$$\bar{E}^{(j)} I \frac{d^2 y^{(j)}}{dx^2} = \frac{Px}{2} \qquad (0 \le x \le L/4) \tag{5}$$

$$\bar{E}_i I \frac{d^2 y_i}{dx^2} = \frac{PL}{8} \qquad (L/4 \le x \le L/2) \tag{6}$$

The elastic modulus of the cantilever can be obtained by solving the above.

$$E_{half} = \frac{11L^3}{384\, C^{(\langle r/4 \rangle)}} \cdot \bar{E}^{(\langle r/4 \rangle)} \tag{7}$$

where $C^{(j)}$ is defined as

Excerpt from ISBN 978-3-00-053387-7

$$C^{(j)} = \begin{cases} \frac{L^3}{192}\left(1-\frac{3}{2}\cdot\frac{\overline{E}^{(1)}}{\overline{E}_{\langle r/4\rangle}}\right)+\frac{\overline{E}^{(1)}}{\overline{E}_{\langle r/4\rangle}}\cdot C_{\langle r/4\rangle} & :\ j=1 \\ \frac{1}{3}\left(1-\frac{\overline{E}^{(j)}}{\overline{E}^{(j-1)}}\right)\left[\frac{L}{4}-(j-1)\sqrt{lw}\right]^3+\frac{\overline{E}^{(j)}}{\overline{E}^{(j-1)}}\cdot C^{(j-1)} & :\ 2\le j\le\langle r/4\rangle \end{cases} \tag{8}$$

C_i is defined as

$$C_i = \begin{cases} \frac{L^3}{32} & :\ i=1 \\ \frac{L}{8}\left(1-\frac{\overline{E}_i}{\overline{E}_{i-1}}\right)\left[\frac{L}{2}-(i-1)\sqrt{lw}\right]^2+\frac{\overline{E}_i}{\overline{E}_{i-1}}\cdot C_{i-1} & :\ 2\le i\le\langle r/4\rangle \end{cases} \tag{9}$$

Finally, flexural modulus along *x*-axis E_1 is calculated by

$$E_1 = \left[\frac{1}{2}\left(\frac{1}{E_{half}^{(1)}}+\frac{1}{E_{half}^{(2)}}\right)\right]^{-1} \tag{10}$$

Moreover, to reproduce the effect of out-of-plane shear deflection, the following expression is added after the calculation of E_1.

$$\frac{1}{E_b} = \frac{1}{E_1}+\frac{12}{11}\left(\frac{T}{L}\right)^2\frac{1}{G_{13}} \tag{11}$$

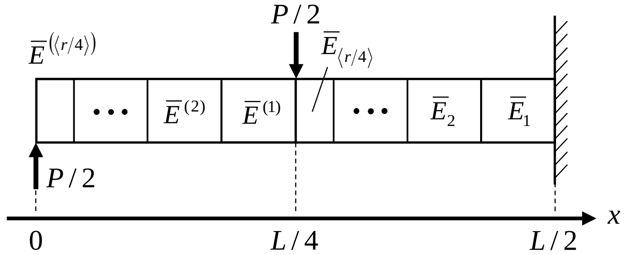

Fig. 2 Half specimen regarded as a cantilever.

2.3. Monte Carlo simulation

These models were constructed by using Monte Carlo simulation in C programing. An orientation angle of an equivalent square ply θ is generated with a random number in the simulations. The plies which have different θ are compounded. The mean μ and variance σ^2 of the flexural modulus can be given by repeating this process *n* times. The inputs are elastic properties of UD tape: E_1, E_2, ν_{12} and G_{12}, G_{13} of UT-CTT; dimension of tape: *t*, *w* and *l*; and dimension of specimen: *T*, *W* and *L*. Elastic properties used for simulation are listed in Table 1. The material is CF/PA6 (polyamide 6) but details will be shown in the next section. Elastic properties of unidirectional material are used as those of CF tape. Specifically, E_1, E_2 and ν_{12} were measured by tensile tests based on ASTM D3039 [11], while G_{12} was measured by tensile tests of $\pm 45°$ laminates based on ASTM D3518 [12]. G_{13} was estimated with the method proposed by Yamashita et al. [13]. The dimension of tape is fixed as *t* = 0.044, *w* = 5 and *l* = 18 mm in this paper because it was reported that tensile strength is saturated at such aspect ratio of tape [14]. The dimension of specimen is determined by test conditions. This simulation takes just a few seconds with a general PC even large *n*, such as ten thousand order.

Excerpt from ISBN 978-3-00-053387-7

Table 1 Elastic properties used in simulation.

	CF UD tape				UT-CTT
CF/PA6	E_1 [GPa]	E_2 [GPa]	ν_{12}	G_{12} [GPa]	G_{13} [GPa]
	125.6	8.0	0.35	3.0	1.11

3. Experiment

3.1. Material fabrication

Prepared ultra-thin prepreg sheet was produced by tow spreading technology [15], which enables the fabrication of the quite thin prepreg, at Industrial Technology Center of Fukui Prefecture. In this study, the fiber and matrix resin were polyacrylonitrile (PAN) – based CF (TR50S, Mitsubishi Rayon Co. Ltd.) and PA6 (Diamiron C®, Mitsubishi Plastics Co. Ltd.), respectively. The thickness of the prepreg was approximately 44 µm and V_f was 55%. It was chopped into $5\,\mathrm{mm}\times 18\,\mathrm{mm}$ tapes and they were dispersed by wet dispersion process. The material was manufactured by compression molding of these dispersed tapes. Details of this manufacturing process can be viewed in previous studies[16,17].

3.2. Bending test

The image of experiment is as shown in Fig. 3. A group of specimens with same specimen thickness, which includes 6 specimens, was prepared. The flexural modulus of each specimen was measured and the mean value and coefficient of variation (CoV) were calculated. Then some groups with various thickness were also prepared. Finally, these mean values and CoV of flexural modulus were compared with results from simulation by analytical models.

The test condition is summarized in Table 2. The dimension of tape was fixed as 0.044 µm in thickness, 5 mm in width and 18 mm in length. Specimen thickness and support span were varied, while width was fixed as 35 mm. Flexural modulus was measured by 3-point bending test and 4-point bending test at a strain rate of 1.0 mm/min.

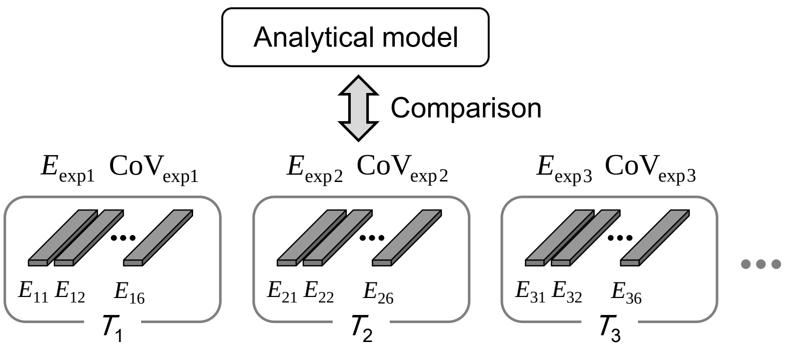

Fig. 3 Image of experimental validation.

Excerpt from ISBN 978-3-00-053387-7

Table 2 Specimens and test conditions.

		Support span [mm]		
		40	60	80
Specimen thickness [mm]	0.47	• Dimension of tape is fixed as t = 0.044, w = 5 and l = 18 mm • Specimen width is fixed as 35 mm. • Number of specimens is fixed as 6. • Both 3-point and 4-point bending test		
	0.79			
	1.08			
	1.58			
	2.02			
	2.89			

4. Results and discussion

Figs. 4 and 5 show the test results. The subscript “calc” and “exp” mean calculation and experiment, respectively. A variable p is the average number of plies, defined as $p = T / t$. The simulation results showed good agreement with experiment and most of mean values of experimental flexural modulus were distributed within $\pm 1\sigma$ range. Flexural modulus was increasing in thin specimen range, while it dropped as the effect of out-of-plane shear deflection became larger. This trend was stronger in short support span. This is because the effect is a function of span-thickness ratio L / T as expression (4) or (11), so it is cleared that test conditions must be considered carefully in bending test of the material with low out-of-plane shear modulus such as UT-CTT. In addition, flexural modulus from 4-point bending was slightly larger than that from 3-point bending, but no significant difference. Therefore, in the case of modulus, 4-point bending test is not much more appropriate than 3-point bending test.

To quantitatively validate models proposed in this study hypothesis testing was performed: The t-test for mean value with the null hypothesis $H_0 : E_{exp} = E_{calc}$ and the χ^2 -test for variance with $H_0 : \sigma^2_{exp} = \sigma^2_{calc}$. The significant level was $\alpha = 0.01$. About mean value, the null hypothesis was accepted except for $L = 40\,\mathrm{mm}, T = 2.89\,\mathrm{mm}$ and $L = 80\,\mathrm{mm}, T = 2.02\,\mathrm{mm}$ in 3-point bending. It was inferred that L / T was so small in the former condition that compression deflection was appeared in addition to bending deflection and out-of-plane deflection because there is stress concentration at the center of the beam in 3-point bending. As for the latter, extremely small CoV probably caused the null hypothesis to be rejected. On the other hand, the null hypothesis was accepted in all conditions about variance. These results of hypothesis testing revealed that the models for flexural modulus show very good agreement with experiment.

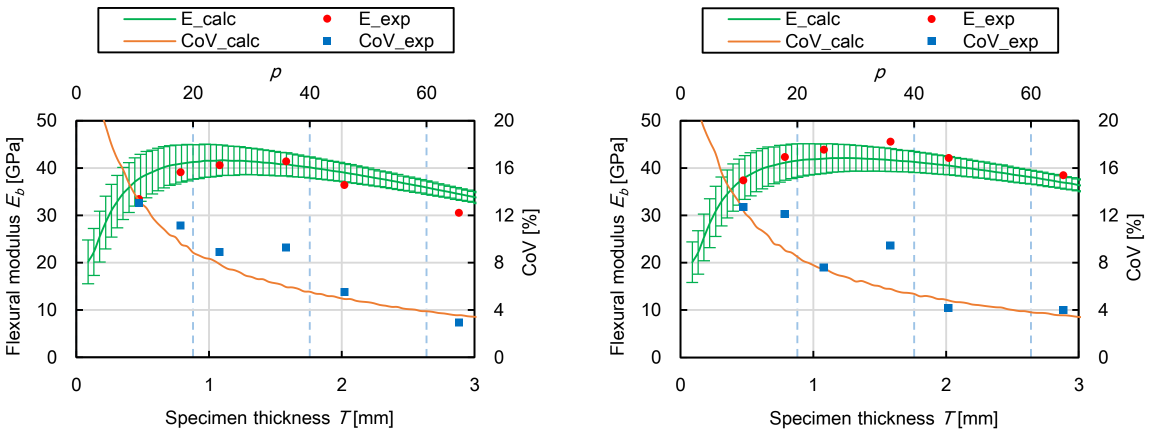

Fig. 4 Results of bending test: L = 40 (left: 3-point bending, right: 4-point bending).

Excerpt from ISBN 978-3-00-053387-7

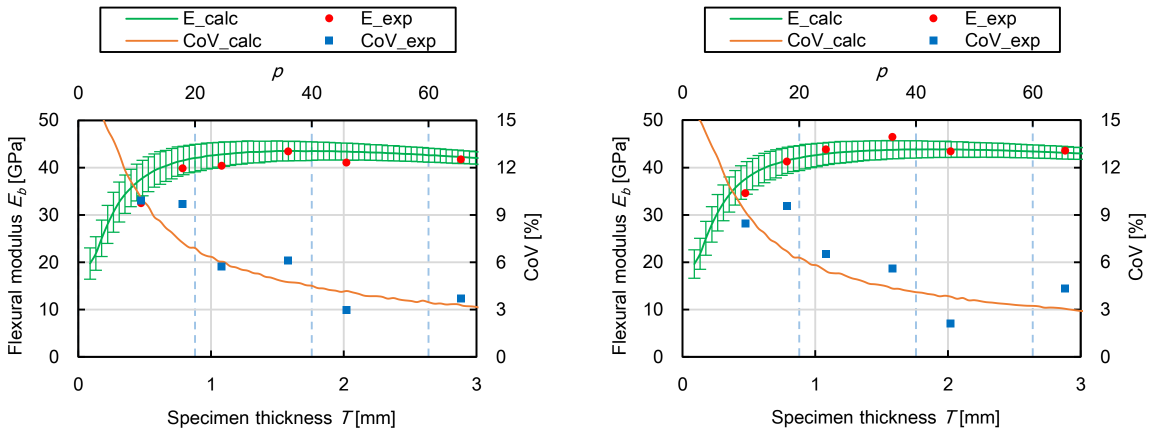

Fig. 5 Results of bending test: L = 80 (left: 3-point bending, right: 4-point bending).

5. Conclusion

UT-CTT, a kind of ROS, is one of the promising material for primary structure of mass-produced automobiles because of its high mechanical properties and suitability for complex shape. However, the relatively large scatter of this material and the low out-of-plane modulus have made it difficult to evaluate properties of actual structures accurately. Thus we discussed about flexural modulus to quantify its scatter and effect of out-of-plane deflection and concluded the following.

- The flexural model of ROS with chopped carbon fiber tapes was constructed as Monte Carlo simulation in two types, 3-point bending and 4-point bending. This simulation outputs a mean value and variance of flexural modulus and is so simple that it takes just a few seconds with a general PC. The prediction results showed good agreement with experiments except for in too short support span and a series of hypothesis testing validated the models.
- In too short support span such as $L < 40$ mm, it was inferred that L/T was so small that compression deflection was appeared in 3-point bending and it made simulations disagree with experiments. Concerning the scatter of elastic properties, there are very small differences between 4-point bending test and 3-point bending test although the scatter of the elastic properties of ROS are decided by the number of strands and strain distribution in a measuring volume. However, 4-point bending test is possible to be useful to obtain the flexural strength of ROS because the scatter of the flexural strength is decided by the number of strands and strain distribution in a measuring surface.

The scatter of flexural modulus was quantified under appearance of out-of-plane shear deflection in this study. It is quite useful for design which took the uncertainty of mechanical properties into consideration. On the other hand, this model assumes no overlap conditions so properties of ROS without water dispersion, in which there can be some waviness, should be concerned in the future work.

Acknowledgments

Part of this study has been conducted as the Japanese METI project "the Future Pioneering Projects / Innovative Structural Materials Project" since 2013fy. The authors would like to express sincere appreciation to the project members who have provided valuable information and useful discussion. In addition, the authors would like to thank Industrial Technology Center of Fukui Prefecture for supplying prepreg sheet.

Excerpt from ISBN 978-3-00-053387-7

References

[1] P. Feraboli, E. Peitso, F. Deleo and T. Cleveland. Characterization of prepreg-based discontinuous carbon fiber/epoxy systems. *Journal of Reinforced Plastics and Composites*, 28:1191-1214, 2009.
[2] A. Levy and P. Hubert. Interstrand void content evolution in compression moulding of randomly oriented strands (ROS) of thermoplastic composites. *Composites: Part A*, 70:121-131, 2015.
[3] B. Landry and P. Hubert. Experimental study of defect formation during processing of randomly-oriented strand carbon/PEEK composites. *Composites: Part A*, 77:301-309, 2015.
[4] P. Feraboli, E. Peitso, T. Cleveland, P.B. Stickler, John C. Halpin. Notched behavior of prepreg-based discontinuous carbon fiber/epoxy systems. *Composites: Part A*, 40:289-299, 2009.
[5] P. Feraboli, T. Cleveland, M. Ciccu, P. Stickler and L. DeOto. Defect and damage analysis of advanced discontinuous carbon/epoxy composite materials. *Composites: Part A*, 41:888-901, 2010.
[6] K. Johanson, L.T. Harper, M.S. Johnson and N.A. Warrior. Heterogeneity of discontinuous carbon fibre composites: Damage initiation captured by Digital Image Correlation. *Composites: Part A*, 68:304-312, 2015.
[7] Y. Sato, J. Takahashi, T. Matsuo, I. Ohsawa, K. Kiriyama and S. Nagoh. Elastic modulus estimation of chopped carbon fiber tape reinforced thermoplastics using the Monte Carlo simulation. *Proceedings of the 19th International Conference on Composite Materials, Montreal*, *Canada*, July 28-August 2, 6718-6725, 2013.
[8] P. Feraboli, T. Cleveland, P. Stickler and J. Halpin. Stochastic laminate analogy for simulating the variability in modulus of discontinuous composite materials. *Composites: Part A*, 41:557-570, 2010.
[9] M. Selezneva, S. Meldrum, S. Roy, L. Lessard and A. Yousefpour. Modeling of mechanical properties of randomly oriented strands thermoplastic composites. *Proceedings of the 16th European conference on composite materials, Seville*, *Spain*, June 22-26, 2014.
[10] X. Zhang. Statistical research on stochastic elastic properties of carbon fiber tape reinforced thermoplastics. *PhD thesis, The University of Tokyo, Japan*, 2015.
[11] ASTM D3039/D3039M-00e1. Standard Test Method for Tensile Properties of Polymer Matrix Composite Materials. ASTM International, 2000.
[12] ASTM D3518/D3518M – 94 (Reapproved 2007). Standard Test Method for In-plane Shear Response of Polymer Matrix Composite Materials by Tensile Test of a ±45°Laminate. ASTM International, 2007.
[13] S. Yamashita, I. Ohsawa, T. Matsuo, X. Zhang and J. Takahashi. Influence of out-of-plane shear modulus on the estimation of flexural modulus of carbon fiber reinforced thermoplastics. *Proceedings of COMPOSITES WEEK, Leuven*, *Belgium*, September 16-20, 2013.
[14] S. Yamashita, K. Hashimoto, H. Suganuma, J. Takahashi, K. Kawabe and T. Murakami. Tape length dependence of the tensile strength of ultra-thin chopped CF tape reinforced thermoplastics. *Proceedings of the 40th Symposium on Japan Society of Composite Materials, Kanazawa, Japan,* September 18-19, No. B1-05, 2015 (in Japanese).
[15] S. Sihn, R. Y. Kim, K. Kawabe and S. W. Tsai. Experimental studies of thin-ply laminated composites. *Composites Science and Technology*, 67:996-1008, 2007.
[16] H. Suganuma, S. Yamashita, X. Zhang, K. Hashimoto, I. Ohsawa and J. Takahashi. Influence of dispersion method to dispersibility and mechanical properties of ultra-thin carbon fiber tape reinforced thermoplastics. *Proceedings of the 20th International Conference on Composite Materials*, *Copenhagen, Denmark*, July 19-24, 2015.
[17] S. Yamashita, Y. Nakashima, J. Takahashi, K. Kawabe and T. Murakami. Tape length dependence of the electrical conductivity of ultra-thin chopped carbon fiber tape reinforced thermoplastics. *Proceedings of the 14th Japan International SAMPE Symposium & Exhibition, Kanazawa, Japan,* December 6-9, 2015.

Excerpt from ISBN 978-3-00-053387-7